Clinical Pharmacokinetics (2025) 64:1811–1825
https://doi.org/10.1007/s40262-025-01573-6

ORIGINAL RESEARCH ARTICLE

Evaluation of Fentanyl-Emerged Adverse Events and Pharmacokinetics in Neonates: A Physiologically Based Pharmacokinetic Modeling Approach

Walaa Yousef Bassyouni Mahdy[1,2] · Kazuhiro Yamamoto[1,3] · Risa Joji[1] · Mari Hashimoto[1] · Ruka Nakasone[4] · Kazumichi Fujioka[4] · Kotaro Itohara[1] · Yumi Kitahiro[1] · Tomohiro Omura[1] · Ikuko Yano[1]

Received: 24 March 2025 / Accepted: 27 August 2025 / Published online: 26 September 2025

Abstract

Background Despite its common use for analgesia in neonatal intensive care units, the optimal dosing and safety profile of fentanyl, particularly regarding suspected fentanyl-emerged adverse events (FEAEs), such as hypotension, desaturation, and oliguria, are not well-defined.

Objective This study aimed to develop an optimal therapeutic monitoring and dosing strategy for fentanyl for neonates. A physiologically based pharmacokinetic (PBPK) model for predicting fentanyl pharmacokinetics across various populations, including preterm and term neonates, was developed, and the relationship between predicted fentanyl exposure and FEAE incidence in neonates was assessed.

Methods A PBPK model was developed and validated against the observed values in the literature. The model's predictive accuracy for fentanyl pharmacokinetics and association with FEAE incidence in an external retrospective cohort of Japanese neonates was evaluated using the predicted concentrations and pharmacokinetic parameters estimated by PBPK simulation.

Results The PBPK model exhibited reasonable predictive performance for serum fentanyl concentrations in actual neonatal patients (mean error: 9.27% [standard error: 5.06%], root mean squared error: 54.7%). The incidence of any FEAE, particularly oxygen desaturation, was associated with the fentanyl concentration-to-dose ratio, but not with some exposure parameters, such as the area under the curve and maximum concentration. The recommended reduced infusion rate allowed serum fentanyl concentrations to fall within the ranges established by the reported values and our data.

Conclusions Our PBPK model and proposed dosing strategy may contribute to safer and more effective fentanyl use in neonates.

Key Points

We developed a model to predict the pharmacokinetics of fentanyl in neonates to aid in determining safer and more effective dosing regimens.

The model demonstrated that specific adverse events during fentanyl administration, such as hypoxia, are associated with the area under the concentration–time curve of fentanyl relative to the administered dose.

By utilizing this model, physicians can tailor fentanyl dosages for each neonate, thereby enhancing analgesic efficacy while minimizing the risk of harmful adverse events.

✉ Kazuhiro Yamamoto
yamakz@okayama-u.ac.jp

1 Department of Pharmacy, Kobe University Hospital, Kobe, Japan

2 Department of Forensic Medicine and Clinical Toxicology, Faculty of Medicine, Assiut University, Asyut, Egypt

3 Department of Integrated Clinical and Basic Pharmaceutical Sciences, Faculty of Medicine, Dentistry and Pharmaceutical Sciences, Okayama University, 2-5-1, Shikata-cho, Kita-ku, Okayama 700-8558, Japan

4 Department of Pediatrics, Graduate School of Medicine, Kobe University, Kobe, Japan

1 Introduction

Fentanyl is the synthetic opioid of choice for analgesia and sedation in neonatal and pediatric intensive care settings [1, 2], prized for its affinity to μ and κ opioid receptors, rapid onset, and capacity to maintain hemodynamic stability without histamine release, even at high doses [3]. The guidelines recommend low-dose continuous infusions of fentanyl during mechanical ventilation to manage pain and stress; however, there is still debate over the best dosing, administration route, and treatment regimen for intensive care unit (ICU) patients [4]. In many countries, fentanyl is frequently used off-label in ICU patients aged < 2 years, despite being officially approved for perioperative analgesia only in children over this age [5]. The off-label use of fentanyl in unstable preterm infants is associated with severe suspected fentanyl-emerged adverse events (FEAEs), including oxygen desaturation, oliguria, and hypercapnia [6], highlighting the urgent need for refined dosing strategies to mitigate risks. The widespread off-label use, coupled with the ethical and practical challenges of conducting pharmacokinetic (PK) studies in pediatric and preterm populations, highlights the critical need for a more profound understanding of fentanyl's PKs in these populations [7].

The PKs of fentanyl in neonates present unique challenges in drug accumulation, even when the dose is adjusted for body size [2]. Current pediatric dosing strategies often rely on linear extrapolation from adult regimens based on weight, a method that fails to account for maturation, particularly differences in drug metabolism and disposition [8]. The development of predictive models that incorporate maturation-dependent changes is crucial for individualizing dosing and enhancing patient outcomes [9]. In particular, the complexity of fentanyl's PK profile is influenced by factors, such as its high protein-binding rate to human serum albumin of > 90% and metabolism by the cytochrome P450 enzyme (CYP) 3A [10]. Furthermore, fentanyl is metabolized to norfentanyl, an inactive metabolite, primarily by CYP3A4 and, to a lesser extent, by CYP3A5 [10]. In neonates, the transition from the fetal CYP3A7 isoform to the adult CYP3A4 isoform shortly after birth [11], along with other maturation changes, complicates the prediction of dosing using adult models. To address these challenges, a physiologically based pharmacokinetic (PBPK) model that accounts for maturation in preterm neonates is useful. PBPK models, which integrate specific demographic factors, drug properties, and PK characteristics, offer a sophisticated and mechanistic alternative to traditional weight-based dosing methods in pediatrics [12].

This study aimed to elucidate the relationships between predicted PK parameters and the incidence of FEAEs to optimize fentanyl dosing strategies in pediatric and neonatal populations. PBPK modeling and simulation were performed to predict fentanyl PKs across various populations, including preterm and term neonates.

2 Materials and Methods

2.1 Software

To construct a comprehensive PBPK model, the Simcyp Population-Based Pharmacokinetic Simulator (version 23; Certara UK Limited, Simcyp Division, Sheffield, UK [13]) was used. The virtual-twin approach, enabled by the Simcyp Simulator V22 Excel Plugin, was used to predict drug disposition in virtual populations. The observed plasma or serum concentration data were extracted from the scientific literature and digitized using WebPlotDigitizer (version 4.4; PLOTCON 2017-Oakland, CA [14]), ensuring adherence to established best practices. Statistical analyses were performed using R (version 3.6.1; R Core Team, 2021) and R Studio (version 2023.09.1-494; R Studio, Inc., Boston, MA, USA, 2021 [15]).

2.2 Development, Verification, and Extrapolation of the Fentanyl PBPK Model

The fentanyl PBPK model was developed using a structured multistep approach that integrated clinical data for broad applicability, including pediatric and preterm populations (Fig. 1). This process involved a Literature review to gather essential parameters and identify relevant studies, ultimately selecting 34 studies for model development and verification (Tables S1–S6). Firstly, the validity of the fentanyl PBPK model was evaluated using the adult population model, incorporating five intravenous drug-drug interaction (DDI) studies to estimate the fraction metabolized (f_m) via CYP3A4 and human liver microsomes (HLM), along with one intravenous administration study evaluating *CYP3A5* polymorphisms to inform CYP3A5-mediated clearance (CL). Physicochemical and PK properties, including molecular weight (MW), blood-to-plasma ratio (B/P), unbound fraction (f_u), steady-state volume of distribution (Vd_{ss}), Kp scalar, and renal clearance (CL_r), were derived from literature sources. Enzyme-specific intrinsic clearance (CL_{int}) for CYP3A4, CYP3A5, and CYP3A7 was calculated using Simcyp's retrograde calculator, incorporating adult clinical PK and DDI data. Next, the validity of the model was evaluated using the pediatric population model provided by Simcyp, which incorporates age-dependent physiological changes, such as hepatic enzyme ontogeny, renal maturation, organ perfusion, and plasma protein binding. The model was verified using clinical studies of pediatric and preterm populations,

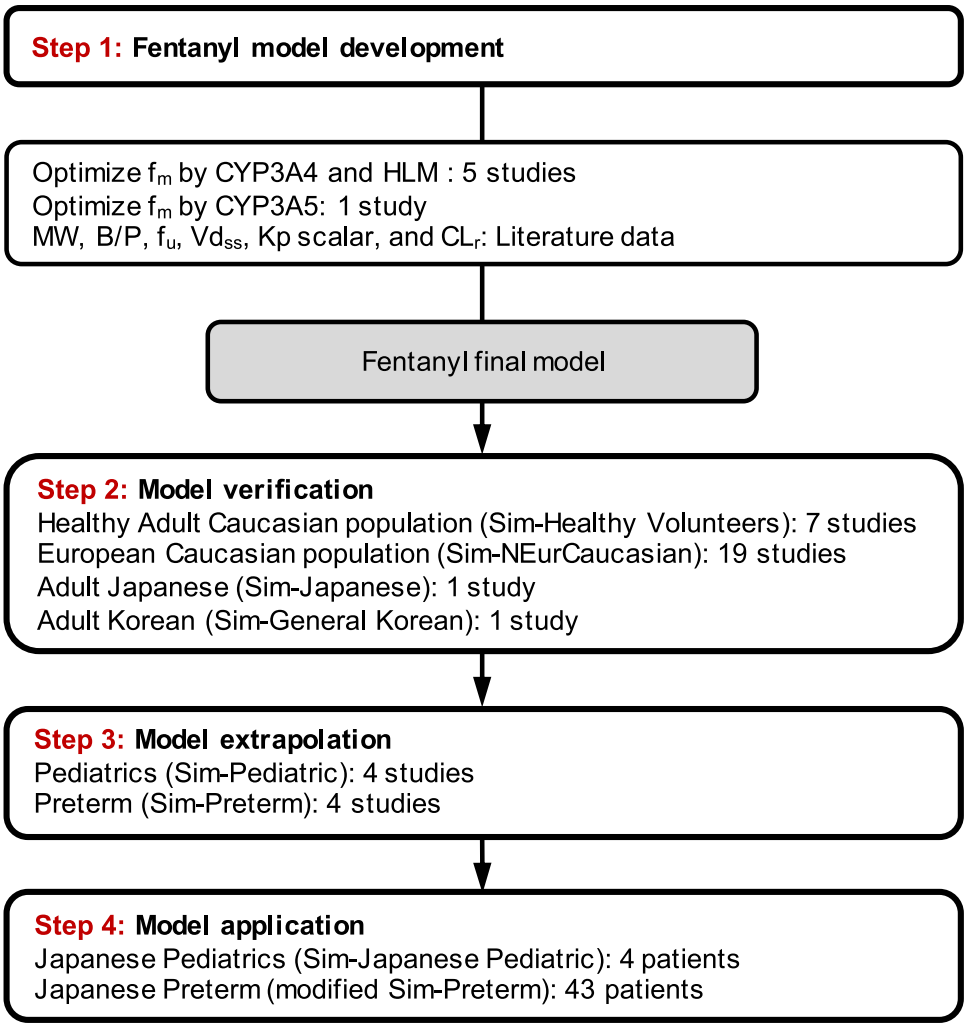

Fig. 1 Schematic workflow of the methodology adopted for fentanyl physiologically based pharmacokinetic (PBPK) model development, verification, extrapolation, and application. The model was developed in adults using literature-based parameters and optimized enzyme contributions, verified across multiple adult populations, and extrapolated to pediatric and preterm populations by incorporating age-dependent physiological changes. The final model was applied to an external Japanese neonatal cohort using a virtual twin simulation approach. f_m fraction metabolized via each enzyme, *HLM* human liver microsomes, *MW* molecular weight, *B/P* blood/plasma concentration ratio, f_u unbound fraction in plasma, Vd_{ss} steady-state volume of distribution, *Kp* scalar, tissue-to-plasma partition coefficients, CL_r renal clearance

particularly focusing on Japanese patients, through a hybrid model of "Preterm model" and "Japanese model" within the Simcyp simulator. Key model parameters were derived from Simcyp system-related factors, such as blood flow rates and organ volumes, and drug-specific characteristics, such as molecular weight and partition coefficients. The model accounted for fentanyl's high hepatic extraction ratio and used enzyme kinetics to predict drug elimination, incorporating intrinsic clearance values for various CYP enzymes involved in metabolism.

The fentanyl PBPK model was evaluated by creating virtual populations that mirrored the demographic information reported in the reference clinical studies using the virtual-twin approach. In cases in which specific adult data were unavailable, a default virtual population of 300 healthy adults aged 18–65 years was used. The initial model evaluation used visual predictive checks, overlaying the mean observed (C_{obs}) and predicted (C_{pred}) systemic fentanyl concentration profiles, along with the 5th–95th percentile prediction ranges. The observed-to-predicted concentration ratios (C_{obs}/C_{pred}) were calculated to assess the model's accuracy. The verification criteria were met when the observed values fell within the 90% prediction interval of the virtual population and the C_{obs}/C_{pred} ratio was within a two-fold difference [16]. Goodness-of-fit (GOF) plots were used to visually compare the C_{pred} with the C_{obs}.

2.3 Clinical Application of the PBPK Model to Neonate Patients

2.3.1 Study Design

This retrospective observational cohort study was conducted in accordance with the Declaration of Helsinki and approved by the Ethics Committee of Kobe University Hospital (approval No. B210177). Data were collected from 1 January 2017 to 31 December 2020.

2.3.2 Inclusion and Exclusion Criteria

The inclusion criteria were as follows: neonates admitted to the neonatal ICU (NICU) of Kobe University Hospital between 1 January 2017 and 31 December 2020; those who required mechanical ventilation; those who were administered fentanyl for sedation; those with complete demographic data; and those who had a gestational age (GA) of ≥ 25 weeks because preterm neonates with a GA of < 25 weeks are considered extremely premature and may have significantly different physiological characteristics and potentially different drug responses compared with more mature neonates. The exclusion criteria were as follows: patients whose parents or persons with parental authority opted out of participation due to their refusal to allow their information to be made publicly available.

2.3.3 Serum Sampling and Fentanyl Concentration Measurement

Residual serum specimens collected for routine laboratory tests and stored for future research purposes were used as samples for measuring fentanyl concentration and were analyzed using liquid chromatography-tandem mass spectrometry at LSI Medience Corporation (Tokyo, Japan). The sample was stored at – 20 °C until measuring fentanyl concentration.

2.3.4 Application of the Fentanyl PBPK Model

To simulate fentanyl concentrations in each Japanese neonatal patient, a "virtual twin" model was developed in which the individual parameters of actual Japanese patients were incorporated into the constructed model. This model incorporated specific variables obtained from electronic medical records (EMRs), including age, sex, body weight, height, and actual dosing information, such as any boluses administered. Concomitant medications (e.g., phenobarbital, diazepam, midazolam, hydrocortisone, dopamine, dobutamine, furosemide) were recorded. To optimize the predictive performance of the PBPK model for fentanyl in the neonatal population, two versions of the model were compared: the original model and the parameter estimation (PE) model. The PE model was developed by estimating the human liver microsome (HLM) intrinsic clearance (CL_{int}) parameter in Simcyp. PE optimization was performed using LogNormal distribution, Maximum Likelihood objective function, (Quasi-Random Parameter Estimation Method) as the algorithm, a Monte Carlo sample size of 8, and an acceptance ratio of 0.10.

2.3.5 Definition of Safety and Efficacy Surrogate Markers

We evaluated FEAE as a safety endpoint and emergence from sedation as an efficacy endpoint for fentanyl therapy. FEAEs were evaluated by assessing the values recorded in the EMRs from pulse oximetry for saturation of percutaneous oxygen (SpO_2), urine output measurement for oliguria detection, and electrocardiography for continuous heart rate monitoring. Clinical thresholds were established to define FEAEs potentially associated with fentanyl administration. Desaturation was stratified as mild (SpO_2 88–89%), moderate (85–87%), and severe (85%), in accordance with oxygen saturation targets for neonates [17–19]. Hypotension was defined as a mean arterial pressure (MAP) below the 10th percentile for the infant's PMA [20]. Moreover, urine output < 1 mL/kg/h after 24 h of birth, and heart rate < 100 bpm were considered as FEAE. Emergence from sedation was defined as body movements and eye opening owing to offset of fentanyl effect after discontinuation of fentanyl administration.

2.4 Dosing Strategies for Fentanyl in Neonates

We applied a structured five-step methodology to establish a target fentanyl concentration range for therapeutic drug monitoring (TDM) and to evaluate the adequacy of current dosing regimens in neonates (Fig. S1). First, the lower limit of the therapeutic window was determined by analyzing fentanyl concentrations at the time of emergence from sedation, used as a surrogate marker of offset of fentanyl effect. Second, the upper limit was defined through (1) a literature review identifying fentanyl concentrations associated with both analgesic efficacy and early adverse events, and (2) AUROC analyses assessing the relationship between fentanyl exposure metrics and FEAEs. The concentration-to-dose ratio (CDr) was calculated for all patients by dividing the area under the curve from time 0 to the end of the infusion ($AUC_{0\text{-end}}$) by the infusion rate multiplied by the duration (t).

$$\mathrm{CDr} = \frac{\mathrm{AUC}_{0-\mathrm{end}}(\mathrm{ng/mL} \cdot \mathrm{h})}{\text{Total dose}(\mu g/\mathrm{kg})}$$

Third, the efficacy of the standard fentanyl dosing regimen (loading dose of 0.5–4 μg/kg followed by 0.5–3 μg/kg/h infusion) was assessed by simulating its performance in maintaining fentanyl concentrations within the identified target range across different GA groups. If the standard regimen is found to be inadequate, an alternative dosing regimen should be proposed to optimize fentanyl dosing for effective analgesia while minimizing the incidence of FEAEs in neonates.

2.5 Statistical Analysis

Descriptive data were reported using appropriate measures, and nonparametric tests were used due to the small sample size. Prediction bias and precision were quantitatively evaluated using the mean error percentage (ME%) ± standard error (SE) and root mean square error (RMSE%), respectively. The ME% is calculated as the average percentage difference between the observed and predicted values. These metrics were calculated using the following equations:

$$\mathrm{ME}(\%) = 100 * \frac{1}{n}\sum_{i=1}^{n}\left(\frac{(\text{Observed value}, i - \text{Simulated value}, i)}{\text{Observed value}, i}\right)$$

$$\mathrm{RMSE}(\%) = 100 * \sqrt{\frac{1}{n}\sum_{i=1}^{n}\left(\frac{(\text{Observed value}, i - \text{Simulated value}, i)}{\text{Observed value}, i}\right)^2}$$

where n is the number of observations of each patient; the observed value i is the actual observed concentration from the clinical data for the ith observation; and the simulated value i is the predicted concentration from the model for the ith observation of each patient. The use of PK parameters in predicting FEAEs in newborn infants was assessed using the area under the receiver operating characteristic curve (AUROC), alongside the determination of various cutoff values.

3 Results

3.1 Building of the PBPK Model and Verification of Adult Model Performance

The developed PBPK model exhibited robust predictive performance for fentanyl PKs in adults following intravenous administration throughout the dosage range (2.78–11.4 mg), including both bolus doses and infusions. The model predictions were closely related to the observed fentanyl concentrations from clinical studies, with all observed systemic concentrations falling within the 90% prediction interval of the predicted data (Figs. S2a–c). Further analysis was performed using GOF plots, which compared C_{pred} and C_{obs}. The GOF plots revealed that 100% of the predicted values satisfied the two-fold acceptance criterion, indicating the model's robust predictive performance (Fig. S2d). The accuracy and precision indexes were found to be ME% ± SE of 1.40% ± 1.28% and an RMSE% of 22.1%, respectively. To evaluate the predictive performance of the developed PBPK model, the simulated PK parameters were compared with the observed data from previously published clinical studies in adults [2, 21–28]. The mean observed total clearance (CL_t) from the Literature was 67.0 ± 15.0 L/h, whereas the PBPK model predicted a CL_t of 53.5 L/h in adults, which falls within 1 SD of the observed mean. Similarly, the predicted volume of distribution at a steady-state (Vd_{ss}) of 9.83 L/kg was closely related to the mean observed value of 8.54 ± 2.45 L/kg in the clinical studies.

3.2 Pediatric and Preterm PBPK Model Extrapolation

The extrapolation of the adult PBPK model to pediatric populations, ranging from 1-day postnatal age (PNA) to 9 years, is shown in Figs. 2a and b. GOF plots confirmed that 97.4% of the predicted serum fentanyl concentrations in pediatric patients adhered to the two-fold acceptance criterion (Fig. 2c). The ME% ± SE and RMSE% values were −8.72% ± 5.94% and 36.2%, respectively. For the Caucasian preterm subgroup, 90.4% of the predicted fentanyl concentrations fell within the two-fold range. The ME% ± SE of 10.2% ± 10.2% and RMSE% of 52.0% for this subgroup indicate a slightly higher bias than the broader pediatric population.

3.3 Fentanyl Metabolism, Elimination Pathways, and PK Maturation

According to the PBPK mass balance simulation, Simcyp estimated the CYP3A to account for the metabolism of 59.7% of the fentanyl dose in adults (Table 1). This fraction exhibited an increase with growth. Notably, a non-specific hepatic pathway was responsible for eliminating approximately 31.6% of the administered dose in adults, and the model estimated that 8.70% of the fentanyl dose was excreted unchanged in the urine. On one hand, Fig. 2d illustrates the maturation of fentanyl PKs as the GA progresses. A notable increase in both CL_t and hepatic clearance (CL_h) from GA25 to GA40 was observed, with CL_t rising from 0.88 to 3.15 L/h and CL_h rising from 0.86 to 2.93 L/h. The CL_r slightly increased across the GAs, and the clearance per kilogram ($CL_{/kg}$) was almost constant. Enzymatic intrinsic activities crucial for fentanyl metabolism, particularly HLM and CYP3A4, increased with GA, whereas CYP3A7 activity was almost constant (Fig. 2e). The CL_{int} of CYP3A5 was as low as that of CYP3A7 and showed almost constant with GA.

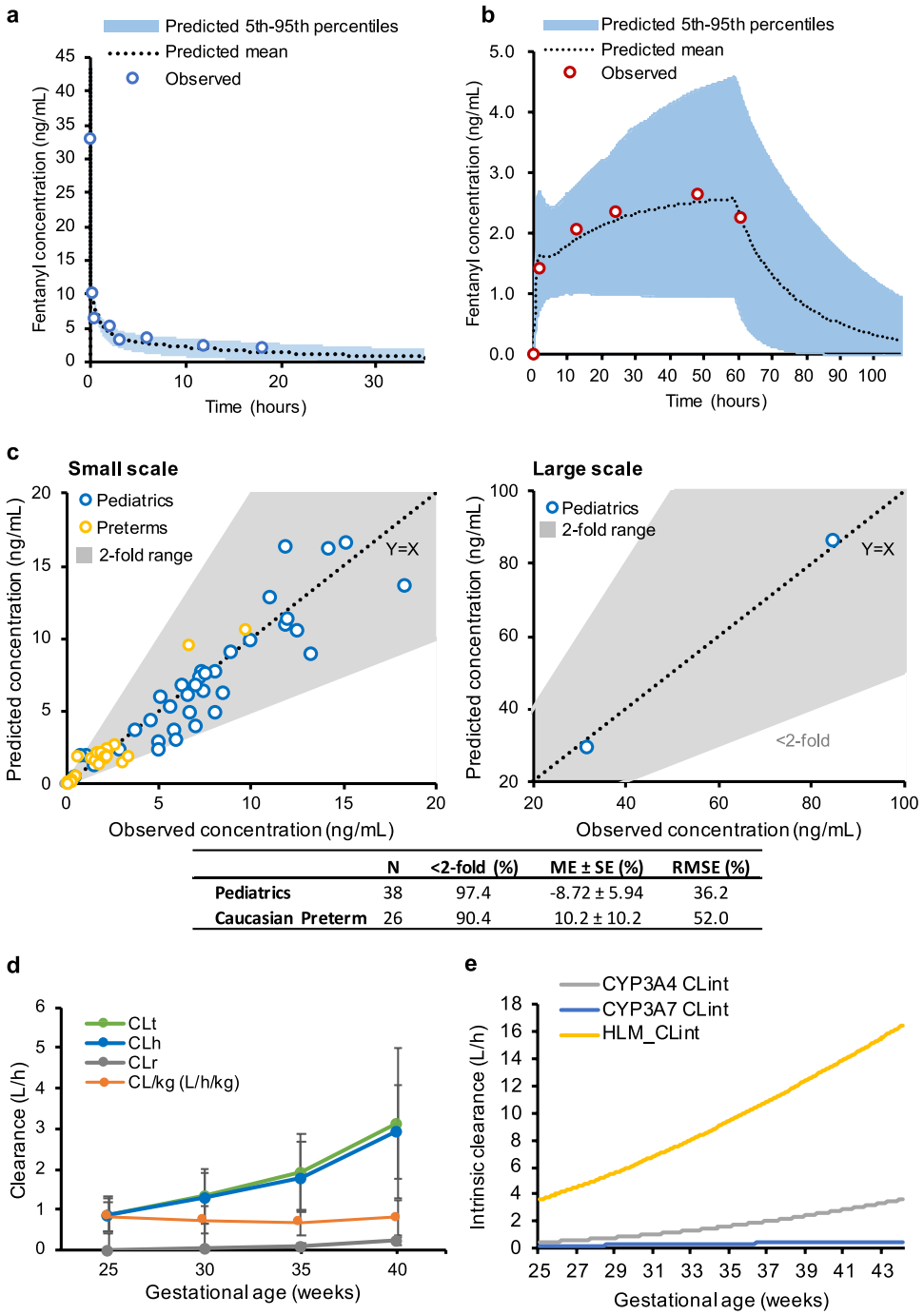

	N	<2-fold (%)	ME ± SE (%)	RMSE (%)
Pediatrics	38	97.4	-8.72 ± 5.94	36.2
Caucasian Preterm	26	90.4	10.2 ± 10.2	52.0

Fig. 2 Model extrapolation to the pediatric and preterm populations. **a** Visual predictive check for physiologically based pharmacokinetic (PBPK) simulation for a pediatric patient following a fentanyl dose of 50 µg/kg [57] and **b** 38 preterm patients from one study after a fentanyl loading dose of 10.5 µg/kg over 1 h, followed by a continuous infusion at 1.5 µg/kg/h [58]. The blue shaded area represents the 5th–95th percentile range, with the dashed black line showing the simulation's mean fentanyl concentration. Open circles indicate observed mean plasma fentanyl concentrations. **c** Scatter plot comparing predicted fentanyl concentrations with the observed fentanyl concentrations across seven preterm and pediatric clinical studies [57–64]. The dashed black Line represents the Line when the observed value is equal to the predicted value. The small-scale graph shows the 0–20 ng/mL concentration range, and the large-scale graph shows the 20–100 ng/mL concentration range. The table in **c** presents the quantitative indicators of prediction bias and precision shown by the mean error percentage (ME%) ± standard error (SE) and the root mean square error (RMSE%), respectively. **d** Association between fentanyl clearance (CL) parameters and neonatal GA groups. This analysis categorized the neonates into GA groups of 25, 30, 35, and 40 weeks. **e** Association between fentanyl intrinsic clearances (CL_{int}) and neonatal GA groups. This scatter plot illustrates the relationship between the GA of neonates and the CL_{int} of fentanyl, including additional hepatic HLM CL_{int}, CYP3A4 CL_{int}, and CYP3A7 CL_{int}. CL_h hepatic clearance, CL_r renal clearance, $CL_{/kg}$ clearance per kg

Table 1 Fractional contributions of different metabolic pathways to fentanyl elimination across gestational ages, pediatric, and adult populations as predicted by the Simcyp simulator

GA	fm_{CYP3A4}	fm_{CYP3A5}	fm_{CYP3A7}	$fm_{Additional\ HLM}$	fe_{renal}
GA25	11.4 ± 8.4	2.18 ± 3.63	4.63 ± 2.27	78.3 ± 11.7	3.49 ± 2.93
GA30	12.7 ± 9.2	2.44 ± 4.01	3.87 ± 1.85	75.8 ± 12.6	5.14 ± 4.20
GA35	14.0 ± 9.8	2.66 ± 4.34	3.16 ± 1.48	73.4 ± 13.4	6.81 ± 5.38
GA40	23.9 ± 20.3	4.20 ± 7.58	1.96 ± 1.49	62.7 ± 21.3	7.27 ± 6.00
Pediatric	40.1 ± 16.6	3.50 ± 11.02	0.11 ± 0.18	43.8 ± 18.6	12.5 ± 11.6
Adult	55.9 ± 16.3	3.78 ± 9.22	0.04 ± 0.14	31.6 ± 16.7	8.70 ± 3.18

The values are shown as mean ± standard deviation (SD)

GA gestational age, *fm* fraction of metabolism, *fe* fraction of elimination

3.4 Application of the PBPK Model to Actual Patients

During the study period, 52 patients received intravenous fentanyl administration in the NICU. One patient was excluded due to incomplete demographic data, and four were excluded due to a GA of less than 25 weeks. Therefore, 47 patients were finally included in the analysis of FEAEs. Furthermore, six patients were excluded owing to the lack of a serum sample, resulting in 41 patients (4 terms and 37 preterms) being included in the PBPK model application step. Figure 3 presents GOF plots for our Japanese population, categorized according to GA, along with a table presenting performance metrics of the original and PE PBPK models during the application step. The predictions from the original PBPK model revealed that 90.4% of the estimated fentanyl concentrations were within the two-fold range with an ME% ± SE of 16.0% ± 6.2% and an RMSE% of 68.4%. In contrast, the PE model, which adjusted the HLM CL_{int} from 73.8 to 66.7 µL/min/mg protein, exhibited enhanced predictive accuracy. This modification reduced the ME% ± SE to 9.27% ± 5.06% and decreased the RMSE% to 54.7%. Of the 21 data points that exceeded the two-fold criterion, 15 were observed after the end of the infusion period. On the basis of these results, the PE model was used in subsequent experiments as the final model. Exploratory analysis in 41 neonates showed a nonsignificant trend toward higher fentanyl concentrations with increasing GA and phenobarbital co-administration. However, neither factor reached statistical significance.

3.5 Association Between Fentanyl PK Parameters and FEAEs

In this cohort of 47 patients, 76.6% experienced at least one FEAE. Hypotension was the most frequently observed FEAEs, occurring in 22 patients (46.8%), followed by desaturation in 20 patients (42.6%), oliguria in 10 patients (21.3%), and bradycardia in four patients (8.5%).

Figure S3 presents the predicted fentanyl concentrations, observed concentrations, and time points of FEAEs onset for each patient. FEAEs were observed across a wide range of fentanyl concentrations. Specifically, hypotension occurred at concentrations ranging from 0.23 to 3.50 ng/mL, while desaturation was observed at concentrations between 0.30 and 3.20 ng/mL. Oliguria occurred between 0.16 and 4.38 ng/mL. No significant demographic differences were identified between patients with and without FEAEs (Table 2). Our analysis indicated that the maximum concentration (C_{max}), its corresponding time (T_{max}), and $AUC_{0\text{-end}}$ of patients without any FEAEs were significantly higher than the predicted concentration at the time of incidence of FEAE ($C_{incidence}$), time to FEAE incidence ($T_{incidence}$), and AUC from time 0 to the time of AE incidence ($AUC_{0\text{–incidence}}$) of patients with any FEAEs, because almost all FEAEs occurred early after the start of fentanyl infusion. Patients with severe desaturation had significantly higher CDr values, with median CDr values of 1.71, than 1.21 for those without it ($p = 0.003$) (Fig. 4). CDr emerged as the PK parameter with the highest AUROC for predicting the occurrence of FEAEs in neonates. Using a CDr cutoff value of 1.38 (ng/mL•h)/(µg/kg), the analysis revealed that patients with a CDr above this threshold were significantly more likely to experience any FEAEs ($p = 0.026$) (Table 3). Furthermore, 80% of patients with a CDr > 1.38 experienced oxygen desaturation, whereas only 25% of those with a CDr < 1.38 experienced oxygen desaturation ($p = 0.001$). However, no significant differences were observed for hypotension and oliguria when stratified by the CDr cutoff. The cutoff C_{max} value was 1.73 ng/mL, with an AUROC of 60.1% for predicting the occurrence of any FEAEs.

3.6 Recommended Infusion Rate and TDM Strategy

The median fentanyl concentration upon the time of emergence from sedation was 0.56 ng/mL (interquartile range [IQR] 0.16–1.02 ng/mL), which serves as the lower limit (0.60 ng/mL) for the therapeutic range of fentanyl in neonates (Fig. 5). An upper Limit of 1.40 ng/mL was established based on a literature review [29–31] and on the present AUROC analysis for FEAEs (Table 3). A previous study indicated that

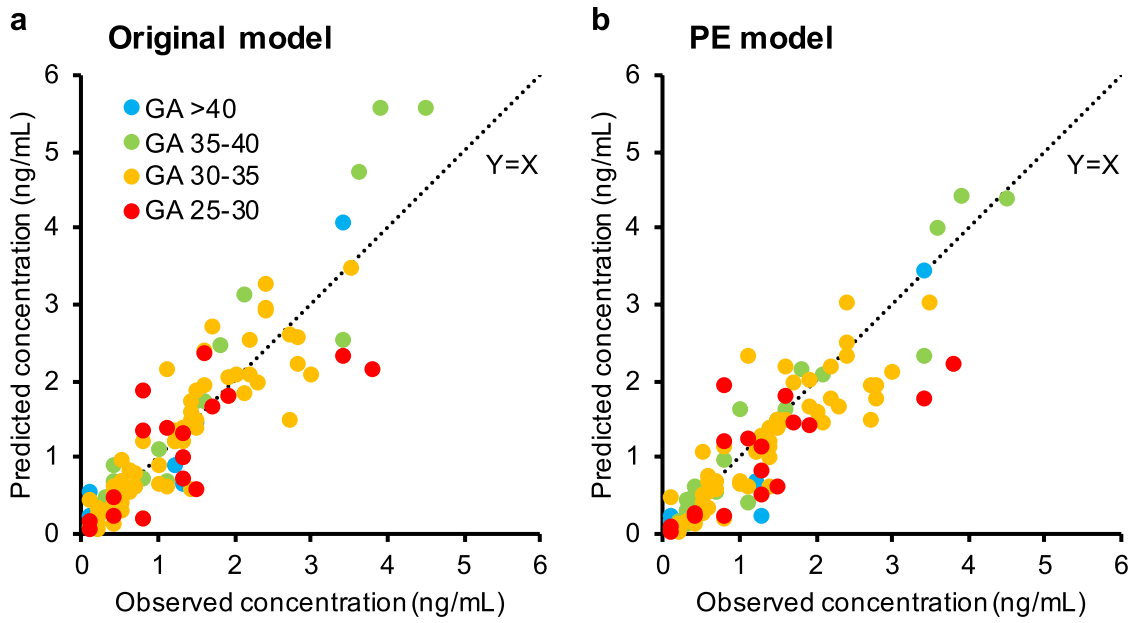

	<2 fold (%)	ME ± SE (%)	RMSE (%)
Original model	90.4	16.0 ± 6.2	68.4
PE model	81.7	9.27 ± 5.06	54.7

Fig. 3 Relationship between the observed and predicted fentanyl serum concentrations from the original and parameter estimation model by gestational age in the application step. This scatter plot shows the correlation between the observed and predicted fentanyl serum concentrations from the original (**a**) and parameter estimation model (**b**) in our study cohort, stratified into gestational age (GA) groups: 25–30, 30–35, 35–40, and > 40 weeks. The dashed lines represent the line when the observed value is equal to the predicted value. Each colored dot corresponds to an individual neonate's concentration–time profile, with colors indicating specific GA categories. The table presents the performance metrics of the physiologically based pharmacokinetic model during the application step

fentanyl concentrations of 1.50–3.00 ng/mL were associated with a 50% depression of CO_2 responsiveness, with hypoventilation occurring in 15% of patients at levels > 1.75 ng/mL [29]. In particular, at 1.40 ng/mL, a 50% decrease in pain intensity was observed with a 12% reduction in minute ventilation, which increased to 23% at 3.0 ng/mL [30]. Furthermore, this upper Limit was well below the potentially toxic concentrations > 2.00 ng/mL suggested cited by the International Association of Forensic Toxicologists (TIAFT) [31]. The CDr threshold for the incidence of any events was 1.38 (ng/mL•h)/(μg/kg) (Table 3). Given that CDr can be interpreted as the concentration per unit infusion rate, assuming a continuous infusion rate of 1 μg/kg/h as the standard dosing, this corresponds to an approximate concentration threshold of 1.40 ng/mL for the incidence of AEs. In addition, a cutoff C_{max} value of 1.73 ng/mL was estimated for predicting the occurrence of any FEAEs in this population, as mentioned above.

The standard fentanyl regimen assessed for GAs between 25 and 40 weeks comprised a loading dose of 2 μg/kg, followed by a continuous infusion of 1 μg/kg/h over 40 h, which was the median duration of fentanyl infusion in the studied cohort (Fig. 6a). This regimen resulted in a C_{max} range of 1.45–1.56 ng/mL. A dosing rate adjustment to a loading dose of 2 μg/kg, followed by a continuous infusion of 0.85 μg/kg/h over 40 h, was simulated (Fig. 6b), resulting in a C_{max} range of 1.23–1.32 ng/mL.

4 Discussion

In this study, a preterm and pediatric PBPK model was successfully developed using the Simcyp Simulator to predict PK for intravenous fentanyl infusion. In this study, the primary concern was the use of the predicted PK parameters from individual patients' clinical characteristics to investigate the relationship between them and the occurrence of FEAEs in the neonatal population.

The developed PBPK model exhibited robust predictive performance for fentanyl PKs in adults and was successfully extrapolated to pediatric populations, including preterm and term neonates. Although the model exhibited acceptable predictive performance overall, a slightly

Table 2 Comparison of patient characteristics and pharmacokinetic parameters between newborn infants with and without fentanyl-emerged adverse events

[Median (IQR)]	FEAEs		*p* value
	Without ($n = 11$)	With ($n = 36$)	
GA (weeks)	33.0 (30.3, 36.6)	33.1 (30.7, 36.3)	0.77
PNA (days)	0.15 (0.12, 1.12)	0.24 (0.16, 0.62)	0.34
Height (cm)	39.0 (36.4, 46.0)	43.2 (39.0, 46.6)	0.53
Albumin (g/L)	31.0 (29.5, 33.5)	29.0 (28.0, 32.3)	0.074
SCr (mg/dL)	0.70 (0.60, 0.86)	0.62 (0.57, 0.69)	0.17
BW (kg)	1.94 (1.23, 2.71)	1.89 (1.42, 2.70)	0.73
5-min Apgar score	9 (8, 9)	8.5 (8, 9)	0.56
Total FEN dose (μg/kg)	21.5 (17.4, 53.3)	52.7 (29.4, 91.1)	0.039
FEN infusion rate (μg/kg/h)	1.10 (1.02, 1.40)	1.11 (0.84, 1.32)	0.32
Duration (h)	21.5 (16.4, 42.3)	47.2 (34.4, 81.9)	0.008
C_{max} (ng/mL)	1.51 (1.31, 1.82)	1.89 (1.41, 2.40)	0.32
$C_{incidence}$ (ng/mL)	–	0.86 (0.58, 1.38)	0.003†
T_{max} (h)	18.8 (15.2, 42.3)	37.0 (27.9, 64.9)	0.074
$T_{incidence}$ (h)	–	11.2 (5.7, 17.5)	0.007§
$AUC_{0–end}$ (ng/mL·h)	25.2 (12.7, 62.2)	60.0 (31.5, 144)	0.029
$AUC_{0–incidence}$ (ng/mL·h)	–	4.92 (2.02, 18.0)	0.002*
CDr ((ng/mL·h)/(μg/kg))	1.12 (0.71, 1.21)	1.29 (1.12, 1.57)	0.015

IQR interquartile range, *FEAE* fentanyl-emerged adverse event, *GA* gestational age, *PNA* postnatal age, *SCr* serum creatinine, *BW* body weight, *FEN* fentanyl, C_{max} maximum predicted concentration, $C_{incidence}$ predicted concentration at the time of FEAE incidence, T_{max} time to maximum concentration, $T_{incidence}$ time to FEAE incidence, $AUC_{0–end}$ area under the curve from time 0 to the end of the infusion, $AUC_{0–incidence}$ area under the curve from time 0 to the time of FEAE incidence, C_{ave} average predicted concentration, *CDr* concentration-to-dose ratio

†*p* value compared to C_{max} of the patients without any FEAE

§*p* value compared to T_{max} of the patients without any FEAE

**p* value compared to $AUC_{0–end}$ of the patients without any FEAE

higher bias and worse precision were observed in the neonatal population (ME% ± SE: 10.2% ± 10.2%, RMSE%: 52.0%) than in older pediatric age groups (ME% ± SE: −8.72% ± 5.94%, RMSE%: 36.2%) (Table embedded in Fig. 2c) and adults (ME% ± SE: 1.40% ± 1.28%, RMSE%: 22.1%) (Table embedded in Fig. S2d). This worse prediction in preterm neonates may be attributed to the unique physiological challenges and variability associated with this age group [2].

Traditionally, fentanyl has been considered to undergo primary hepatic metabolism via CYP3A4-mediated N-dealkylation to norfentanyl. However, our PBPK model indicated a substantial additional hepatic metabolic component captured as "additional HLM" that reflects non-CYP3A-mediated metabolism. This pathway accounted for approximately 31.6% of CL_h in adults, and increased to 78.3% at GA25 in preterm neonates (Table 1), highlighting a significant age-dependent change in metabolic routes. This developmental change likely reflects the ontogeny of hepatic enzymes, as CYP3A4 and CYP3A5 are poorly expressed in early life, while carboxylesterases, aldehyde oxidase, and microsomal oxidoreductases are more active in neonates [32–34]. The role of non-CYP enzymes is further supported by the metabolism of related opioids like remifentanil, which undergoes esterase-mediated hydrolysis [34]. Our adult model estimated the proportion of non-CYP3A metabolism to be 31.6%, which is lower than estimates reported in previous PBPK models [35, 36]. Unlike those models, we explicitly distinguished CYP3A4 and CYP3A5 contributions using DDI data [22–26] and *CYP3A5* pharmacogenetic data [23, 37], allowing for a more precise mechanistic allocation of fentanyl CL, which we believe enabled a reduction in reliance on lumped residual terms. This stratification is especially important in pediatric populations where enzyme ontogeny varies markedly.

The results presented in Fig. 2d provide critical insights into the developmental fentanyl PKs, revealing significant changes in fentanyl disposition during fetal development. The observed increase in both CL_t and CL_h with advancing GA may be based on physical growth because $CL_{/kg}$ was constant, regardless of GA progress. This implies that fentanyl PK changes based on physical growth rather than organ maturation. This observation is particularly relevant for our study cohort, which predominantly consisted of very preterm neonates (GA < 37 weeks), a population known to have minimal hepatic CYP3A4/5 activity. As shown in Fig. 2e, CL_{int} values

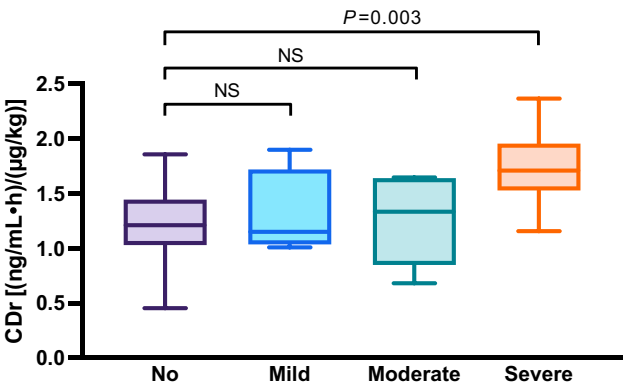

Fig. 4 Association between fentanyl concentration-to-dose ratio (CDr) and oxygen desaturation severity. The *x*-axis categorizes the severity of oxygen desaturation, whereas the *y*-axis represents the CDr values. The boxes represent the interquartile range of CDr for each desaturation category, with the horizontal line within each box denoting the median CDr value. The *p* values positioned above the boxes indicate the statistical significance of the comparisons between CDr levels in patients without adverse events and those with varying severity levels of desaturation using Dunnett's test

Table 3 Cutoff values of concentration-to-dose ratio for each fentanyl-emerged adverse event, and incidence of each event using the cutoff value of 1.38 (ng/mL·h)/(μg/kg)

FEAE	Cutoff ((ng/mL·h)/(μg/kg))	AUROC (%)	Incidence, *n* (%)		*p* value
			CDr < 1.38 (*n* = 32)	CDr ≥ 1.38 (*n* = 15)	
Any events	1.38	74.5	21 (65.6)	15 (100)	0.026
Hypotension	1.04	70.7	12 (37.5)	10 (66.7)	0.12
Oxygen desaturation	1.42	78.3	8 (25.0)	12 (80.0)	0.001
Oliguria	1.16	70.0	5 (15.6)	5 (33.3)	0.32

FEAE fentanyl-emerged adverse event, *AUROC* are under the receiver operating characteristic curve, *CDr* concentration-to-dose ratio

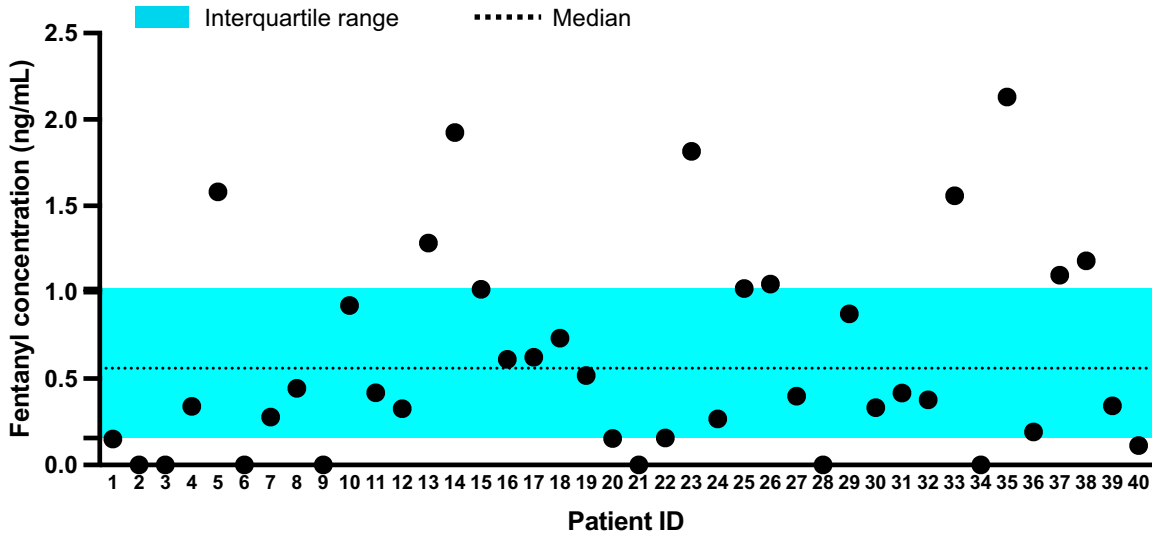

Fig. 5 Fentanyl concentration upon the time of emergence from sedation in neonates. This scatterplot depicts the distribution of fentanyl serum concentrations upon the time of emergence from sedation among a cohort of Japanese neonates (n = 40). The median concentration is marked by a dashed horizontal Line at 0.56 ng/mL, and the interquartile range from 0.16 to 1.02 ng/mL is shaded in blue. Each circle represents an individual neonate's fentanyl concentration

for CYP3A4 and HLM showed increasing trends with advancing GA, reflecting significant physical growth in fentanyl PKs in neonates. A previous report demonstrated that fentanyl has a high hepatic extraction ratio. For drugs with high extraction ratios, CL_h is primarily dependent on hepatic blood flow rather than on CL_{int} and f_u. Hepatic blood flow increases with physical growth. However, the hepatic extraction ratio in neonates was lower than that in the adult population [38]. A lower hepatic extraction ratio due to low birth weight, surgery, or cardiac disease causes a change in the dependency of CL_h from hepatic blood flow to CL_{int}. Furthermore, drugs such as theophylline and phenobarbital, which are also administered to neonates, have low liver extraction rates. In these cases, the impact of CL_{int} on CL_t may be relatively high. Therefore, the relative stability of $CL_{/kg}$ across GA should not be interpreted as an absence of developmental change in PKs, but rather as a reflection of the unique ontogeny of CYP3A enzymes and the predominance of structural and circulatory growth during this phase.

To better reflect the Japanese neonatal population, we applied PE, reducing HLM CL_{int} from 73.8 to 66.7 μL/min/mg protein. The original value was derived using Simcyp's retrograde calculator based on adult clinical PK data, DDI studies to estimate the fraction metabolized (f_m) via CYP3A4 and HLM, and *CYP3A5* poor metabolizer data to calculate CYP3A5-mediated CL, corresponding to enzyme-specific CL_{int} values of 0.864 and 0.548 μL/min/pmol for CYP3A4 and CYP3A5, respectively. While the PE-adjusted model exhibited a slight increase in predictions outside the two-fold error range, these deviations were mainly observed at low concentrations post-infusion which is a known limitation in neonatal PK modeling related to elimination-phase variability [39]. On the basis of a population pharmacokinetic analysis involving 164 neonates, the interindividual variability in systemic clearance of fentanyl was reported to be 44% [33], indicating a highly heterogeneous population. Therefore, the adjustment of HLM CL_{int} by the current

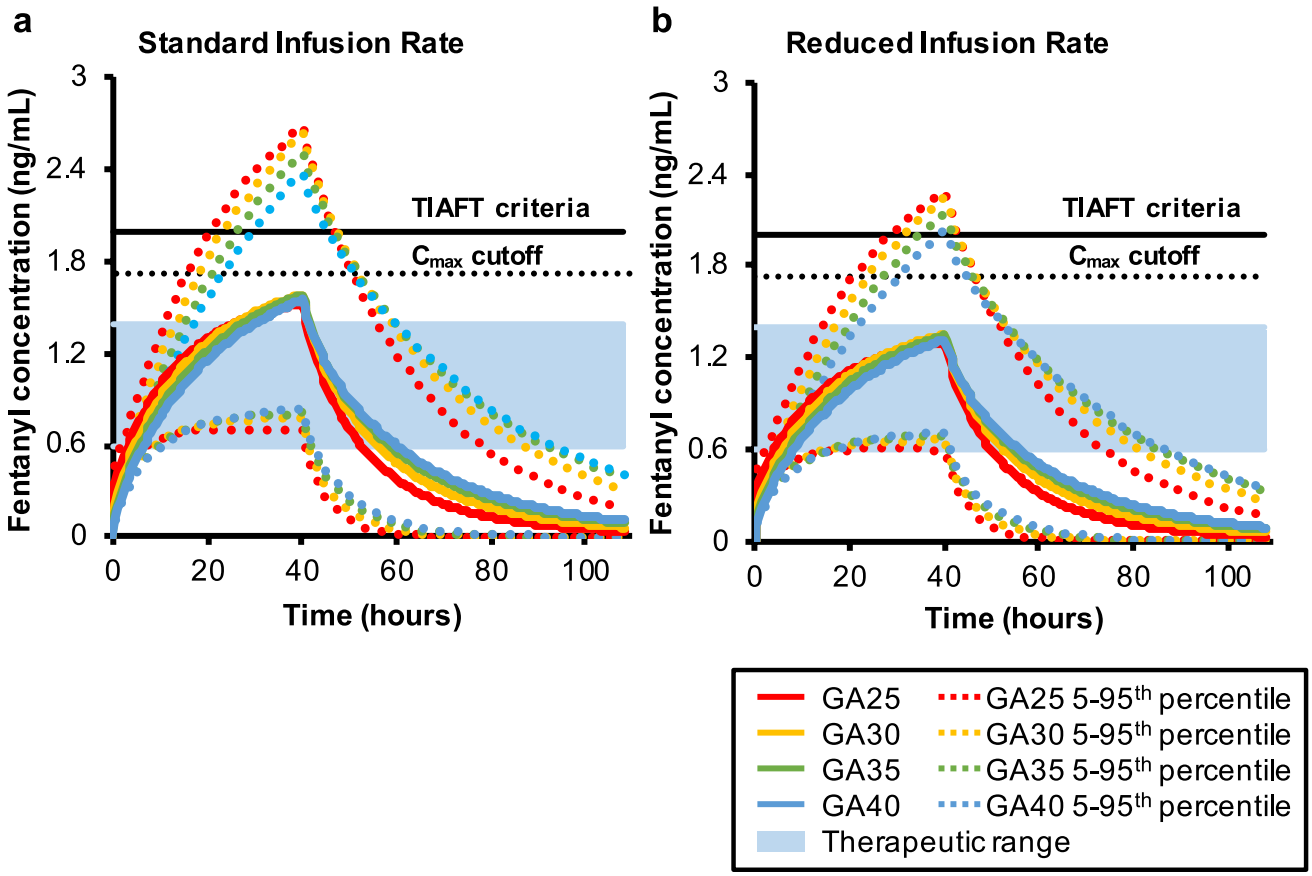

Fig. 6 Physiologically based pharmacokinetic simulation of the standard and reduced fentanyl regimen across the neonatal gestational age groups. Physiologically based pharmacokinetic simulation for **a** the standard fentanyl regimen, which includes a loading dose of 2 µg/kg, followed by a continuous infusion of 1 µg/kg/h over 40 h, and **b** the reduced regimen, which includes a loading dose of 2 µg/kg, followed by a continuous infusion of 0.85 µg/kg/h over 40 h, across neonatal gestational age (GA) groups. The shaded blue area indicates the therapeutic range for fentanyl (0.6–1.4 ng/mL). The colored Lines represent the mean predicted fentanyl concentrations for each GA category. The colored dotted Lines represent the 5th–95th percentile ranges of the predicted fentanyl concentrations for each GA category. The black dotted lines denote the maximum concentration (C_{max}) cut-off value calculated from the present neonates' population. The black solid line denotes the critical pharmacological thresholds suggested by the International Association of Forensic Toxicologists (TIAFT)

PE approach is considered to fall within a reasonable and acceptable range.

In this study, we investigated the relationship between the FEAEs and its PK parameters predicted by our PBPK model in newborn infants. Most FEAEs were noted early during the initiation of fentanyl administration (Fig. S3), highlighting the importance of investigating PKs during the initial drug exposure phase. Notably, CDr values, reflecting the level of increase in AUC per dose, were significantly higher in patients with FEAEs than in those without (Table 2). This suggests that CDr, much like Vd [40], may indicate how readily plasma concentrations rise after drug administration, with higher CDr values likely corresponding to faster increases in serum drug levels, potentially elevating the risk of FEAEs. These findings position CDr as a promising marker for identifying patients at risk of FEAEs, particularly during the early phase of fentanyl therapy. On the other hand, the patients that developed FEAE had the characteristic of a longer treatment duration. One possible explanation is that patients who experience FEAE tend to require longer fentanyl treatment due to poor hemodynamics, and such patients may be more susceptible to FEAE. It cannot be ruled out that not only differences in pharmacokinetic parameters but also this higher susceptibility act as confounding factors. To clearly distinguish these factors and to assert the involvement of PKs, it is necessary to conduct analyses using study subjects with comprehensive data, including multiple fentanyl concentration measurements and background factors such as hemodynamics.

Using a CDr cutoff value of 1.38 (ng/mL•h)/(µg/kg), the analysis revealed that patients with a CDr above this threshold were significantly more likely to experience composite FEAEs

($p = 0.026$), with 100% of these patients reporting FEAEs compared with 65.6% of those below the cutoff (Table 3). Drawing from TDM practices for immunosuppressive, antipsychotic, and antiepileptic drugs, the CDr has emerged as a critical tool for capturing variability in drug metabolism and CL [41–45]. In particular, the patients with severe oxygen desaturation had significantly higher CDr value, as shown in Fig. 4, suggesting a CDr-dependent relationship between how readily blood concentrations rise after drug administration and respiratory depression in neonates, which is consistent with the established facts for different opioids [46]. The relationship between fentanyl concentrations and desaturation aligns with known opioid pharmacology: μ-opioid receptor activation in the brainstem inhibits neuronal excitability and disrupts respiratory rhythm generation (e.g., within the pre-Bötzinger complex), leading to reduced respiratory drive, lower tidal volume, and diminished CO_2/O_2 responsiveness [47–49]. Even under mechanical ventilation, opioids can dampen intrinsic respiratory effort, prolong ventilator dependence, and delay extubation—especially in preterm neonates with immature respiratory control centers [50, 51]. In our cohort, CDr was significantly associated with desaturation, but not with hypotension or oliguria. Although desaturation is multifactorial in etiology and not solely attributable to fentanyl, its association with CDr supports the utility of desaturation as a clinical surrogate for opioid-induced respiratory instability, particularly in neonates with immature central regulation. Interestingly, the lack of a linear relationship between fentanyl dose and desaturation severity highlights the complex interplay between fentanyl PK and physiological outcomes [52].

Establishing an appropriate fentanyl dosing regimen for neonatal patients requires a delicate balance between effective analgesia and minimizing the occurrence of FEAEs, a challenge compounded by the lack of well-defined target concentrations for this vulnerable population [53]. The lower Limit of the target concentration range was set at 0.60 ng/mL, based on the median fentanyl concentration at the time of emergence from sedation. This finding is consistent with that of previous studies that reported that a concentration of 0.60 ng/mL yields slight but measurable analgesia [54]. Other reports have demonstrated that pain relief efficacy reached 100% at approximately 0.60 ng/mL of fentanyl concentration in preterm infants [55]. We explored potential factors contributing to interindividual variability in fentanyl concentrations at the time of emergence from sedation, which was used in this study as a surrogate for the offset of fentanyl effect. While linear regression analyses suggested a trend toward higher fentanyl concentrations at the time of emergence from sedation in infants with greater GA or phenobarbital co-administration, neither factor reached statistical significance in our study population. Given the immaturity of hepatic CYP3A4/5 activity in preterm neonates, the enzyme-inducing effect of phenobarbital is likely attenuated, limiting its PK influence on fentanyl CL. Further investigation is needed to elucidate the factors contributing to the variability in fentanyl concentration at the time of emergence from sedation.

The upper Limit of the target range identified as 1.40 ng/mL by two methods (Fig. S1). The standard fentanyl dosing regimen resulted in a C_{max} range of 1.45–1.56 ng/mL across the different GA groups (Fig. 6a). This standard regimen may result in a C_{max} exceeding the identified therapeutic range. The recommended alternative reduced regimen had a C_{max} range of 1.23–1.32 ng/mL for GAs between 25 and 40 weeks (Fig. 6b). Our simulation indicated that even with this reduced dosing regimen, fentanyl concentrations in some patients still exceeded the therapeutic range. Therefore, measuring fentanyl concentrations and adjusting doses to target therapeutic range 10–20 h after initiating dosing are recommended to adjust the infusion rate accordingly. Nevertheless, this alternative dosing strategy may provide a safer and more effective approach to fentanyl administration in neonatal patients than the standard regimen.

This study has several limitations. First, the neonatal cohort was relatively small, especially among term neonates, which may limit the generalizability of our findings. The retrospective study design could have introduced bias, particularly in the assessment of FEAEs. Second, critical respiratory variables (e.g., fraction of inspired oxygen, mean airway pressure) were not consistently recorded in the EMRs, limiting our ability to evaluate their influence on FEAE. Third, while co-administered therapies and clinical conditions were carefully recorded, their pharmacodynamic or PK interactions with fentanyl were not exhaustively assessed. Finally, the absence of individual pharmacogenetic data—particularly for *CYP3A5*, *CYP3A7*, and key drug transporters such as P-glycoprotein (*ABCB1*)—may have contributed to unexplained interindividual variability in fentanyl metabolism and disposition [37, 56]. Although genotype-based scaling was applied at the population level, the lack of subject-specific genotyping reduces model precision. As evidence grows linking transporter and enzyme polymorphisms to neonatal PKs, future PBPK models should incorporate individual-level pharmacogenetic data to enhance predictive accuracy. Future prospective studies with larger, genotype-characterized cohorts and fully integrated physiologic and PK data are needed to better delineate the multifactorial determinants of fentanyl response and adverse events in neonatal populations.

Our PBPK model showed strong predictive capabilities for fentanyl PKs in both adult and pediatric populations, including preterm and term neonates. The model can help better understand the relationship between fentanyl PKs and FEAE incidence. Our recommended infusion

rates, based on the median fentanyl concentration upon emergence from sedation and the risk of FEAE, may contribute to safer and more effective fentanyl therapy in neonates; however, prospective clinical validation is needed to confirm these findings.

Supplementary Information The online version contains supplementary material available at https://doi.org/10.1007/s40262-025-01573-6.

Acknowledgements We would like to thank our subjects whose data were analyzed in this study.

Funding Open Access funding provided by Okayama University. This work was partly supported by research grants from JSPS KAKENHI (grant numbers 20H00102 and 22K06697) and the Japan Research Foundation for Clinical Pharmacology.

Declarations

Conflict of interest The authors declare no relevant financial or non-financial interests.

Ethics approval This study conformed to the principles of the Declaration of Helsinki. The study protocol was approved by the Ethics Committee of Kobe University Hospital (No. B210177).

Consent to participate Informed consent for participation was obtained using an opt-out approach.

Consent for publication Informed consent for publication was obtained using an opt-out approach.

Availability of data and material All data generated in this study are available from the corresponding author upon reasonable request.

Code availability Not applicable.

Authors' contributions M.W.Y.B. and Y.K. designed and performed simulations of serum drug concentrations, drafted the initial manuscript, and reviewed the manuscript; J.R., H.M., N.R., and F.K. collected data from the neonates and revised the manuscript; I.K., K.Y., and O.T. coordinated and supervised data collection and reviewed and revised the manuscript. Y.I. supervised the conception of this report and interpretation of data and critically revised the manuscript for important intellectual content. All authors read, edited, and approved the final version of this manuscript.

References

1. Pacifici GM. Clinical pharmacology of fentanyl in preterm infants. A review. Pediatr Neonatol. 2015;56:143–8.
2. Ziesenitz VC, Vaughns JD, Koch G, Mikus G, van den Anker JN. Pharmacokinetics of fentanyl and its derivatives in children: a comprehensive review. Clin Pharmacokinet. 2018;57:125–49.
3. Aranda JV, Carlo W, Hummel P, Thomas R, Lehr VT, Anand KJS. Analgesia and sedation during mechanical ventilation in neonates. Clin Ther. 2005;27:877–99.
4. Hughes CG, McGrane S, Pandharipande PP. Sedation in the intensive care setting. Clin Pharmacol Adv Appl. 2012;4:53–63.
5. Fentanyl citrate [package insert]. Hospira Inc. Pfizer Inc; Lake Forest, IL. [Internet]. https://www.accessdata.fda.gov/drugsatfda_docs/label/2016/019115s030s031lbl.pdf. Accessed Dec 2016.
6. Oshikoya KA, Wharton GT, Avant D, Van Driest SL, Fenn NE, Lardieri A, et al. Serious adverse events associated with off-label use of azithromycin or fentanyl in children in intensive care units: a retrospective chart review. Paediatr Drugs. 2019;21:47–58.
7. Ward RM, Sherwin CMT. Ethics of drug studies in the newborn. Paediatr Drugs. 2015;17:37–42.
8. Bellanti F, Della Pasqua O. Modelling and simulation as research tools in paediatric drug development. Eur J Clin Pharmacol. 2011;67(Suppl 1):75–86.
9. Encinas E, Calvo R, Lukas JC, Vozmediano V, Rodriguez M, Suarez E. A predictive pharmacokinetic/pharmacodynamic model of fentanyl for analgesia/sedation in neonates based on a semi-physiologic approach. Paediatr Drugs. 2013;15:247–57.
10. Bista SR, Haywood A, Hardy J, Lobb M, Tapuni A, Norris R. Protein binding of fentanyl and its metabolite nor-fentanyl in human plasma, albumin and α-1 acid glycoprotein. Xenobiotica. 2015;45:207–12.
11. Li H, Lampe JN. Neonatal cytochrome P450 CYP3A7: a comprehensive review of its role in development, disease, and xenobiotic metabolism. Arch Biochem Biophys. 2019;673:108078.
12. Anderson BJ, Holford NHG. Mechanistic basis of using body size and maturation to predict clearance in humans. Drug Metab Pharmacokinet. 2009;24:25–36.
13. Jamei M, Marciniak S, Feng K, Barnett A, Tucker G, Rostami-Hodjegan A. The Simcyp ® population-based ADME simulator. Expert Opin Drug Metab Toxicol. 2009;5:211–23.
14. Wojtyniak J-G, Britz H, Selzer D, Schwab M, Lehr T. Data digitizing: accurate and precise data extraction for quantitative systems pharmacology and physiologically-based pharmacokinetic modeling. CPT Pharmacomet Syst Pharmacol. 2020;9:322–31.
15. R: The R Project for Statistical Computing [Internet]. https://www.r-project.org/. Accessed 29 Feb 2024.
16. Cui C, Valerie Sia JE, Tu S, Li X, Dong Z, Yu Z, et al. Development of a physiologically based pharmacokinetic (PBPK) population model for Chinese elderly subjects. Br J Clin Pharmacol. 2021;87:2711–22.
17. Cayabyab R, Arora V, Wertheimer F, Durand M, Ramanathan R. Graded oxygen saturation targets and retinopathy of prematurity in extremely preterm infants. Pediatr Res. 2016;80:401–6.
18. Chang M. Optimal oxygen saturation in premature infants. Korean J Pediatr. 2011;54:359–62.
19. Sola A, Golombek SG, Montes Bueno MT, Lemus-Varela L, Zuluaga C, Domínguez F, et al. Safe oxygen saturation targeting and monitoring in preterm infants: can we avoid hypoxia and hyperoxia? Acta Paediatr. 2014;103:1009–18.
20. Zubrow AB, Hulman S, Kushner H, Falkner B. Determinants of blood pressure in infants admitted to neonatal intensive care units: a prospective multicenter study. Philadelphia Neonatal Blood Pressure Study Group. J Perinatol. 1995;15:470–9.

21. McClain DA, Hug CC. Intravenous fentanyl kinetics. Clin Pharmacol Ther. 1980;28:106–14.
22. Saari TI, Laine K, Neuvonen M, Neuvonen PJ, Olkkola KT. Effect of voriconazole and fluconazole on the pharmacokinetics of intravenous fentanyl. Eur J Clin Pharmacol. 2008;64:25–30.
23. Ibrahim AE, Feldman J, Karim A, Kharasch ED. Simultaneous assessment of drug interactions with low- and high-extraction opioids: application to parecoxib effects on the pharmacokinetics and pharmacodynamics of fentanyl and alfentanil. Anesthesiology. 2003;98:853–61.
24. Ziesenitz VC, König SK, Mahlke NS, Skopp G, Haefeli WE, Mikus G. Pharmacokinetic interaction of intravenous fentanyl with ketoconazole. J Clin Pharmacol. 2015;55:708–17.
25. Olkkola KT, Palkama VJ, Neuvonen PJ. Ritonavir's role in reducing fentanyl clearance and prolonging its half-life. Anesthesiology. 1999;91:681–5.
26. Palkama VJ, Neuvonen PJ, Olkkola KT. The CYP 3A4 inhibitor itraconazole has no effect on the pharmacokinetics of i.v. fentanyl. Br J Anaesth. 1998;81:598–600.
27. Macleod DB, Habib AS, Ikeda K, Spyker DA, Cassella JV, Ho KY, et al. Inhaled fentanyl aerosol in healthy volunteers: pharmacokinetics and pharmacodynamics. Anesth Analg. 2012;115:1071–7.
28. Streisand JB, Varvel JR, Stanski DR, Le Maire L, Ashburn MA, Hague BI, et al. Absorption and bioavailability of oral transmucosal fentanyl citrate. Anesthesiology. 1991;75:223–9.
29. Cartwright P, Prys-Roberts C, Gill K, Dye A, Stafford M, Gray A. Ventilatory depression related to plasma fentanyl concentrations during and after anesthesia in humans. Anesth Analg. 1983;62:966–74.
30. Nozari A, Akeju O, Mirzakhani H, Eskandar E, Ma Z, Hossain MA, et al. Prolonged therapy with the anticonvulsant carbamazepine leads to increased plasma clearance of fentanyl. J Pharm Pharmacol. 2019;71:982–7.
31. Schulz M, Schmoldt A, Andresen-Streichert H, Iwersen-Bergmann S. Revisited: Therapeutic and toxic blood concentrations of more than 1100 drugs and other xenobiotics. Crit Care. 2020;24:195.
32. Argikar UA, Potter PM, Hutzler JM, Marathe PH. Challenges and opportunities with non-CYP enzymes aldehyde oxidase, carboxylesterase, and UDP-glucuronosyltransferase: focus on reaction phenotyping and prediction of human clearance. AAPS J. 2016;18:1391–405.
33. Wu Y, Völler S, Flint RB, Simons SHP, Allegaert K, Fellman V, et al. Pre- and postnatal maturation are important for fentanyl exposure in preterm and term newborns: a pooled population pharmacokinetic study. Clin Pharmacokinet. 2022;61:401–12.
34. Wilde M, Pichini S, Pacifici R, Tagliabracci A, Busardò FP, Auwärter V, et al. Metabolic pathways and potencies of new fentanyl analogs. Front Pharmacol [Internet]. 2019. https://doi.org/10.3389/fphar.2019.00238/full.
35. Kovar L, Weber A, Zemlin M, Kohl Y, Bals R, Meibohm B, et al. Physiologically-based pharmacokinetic (PBPK) modeling providing insights into fentanyl pharmacokinetics in adults and pediatric patients. Pharmaceutics. 2020;12:908.
36. Mukherjee D, Collins M, Dylla DE, Kaur J, Semizarov D, Martinez A, et al. Assessment of drug–drug interaction risk between intravenous fentanyl and the glecaprevir/pibrentasvir combination regimen in hepatitis C patients using physiologically based pharmacokinetic modeling and simulations. Infect Dis Ther. 2023;12:2057–70.
37. Williams ML, Kannankeril PJ, Breeyear JH, Edwards TL, Van Driest SL, Choi L. Effect of CYP3A5 and CYP3A4 genetic variants on fentanyl pharmacokinetics in a pediatric population. Clin Pharmacol Ther. 2022;111:896–908.
38. Kuhls E, Gauntlett IS, Lau M, Brown R, Rudolph CD, Teitel DF, et al. Effect of increased intra-abdominal pressure on hepatic extraction and clearance of fentanyl in neonatal lambs. J Pharmacol Exp Ther. 1995;274:115–9.
39. Dinh J, Johnson TN, Grimstein M, Lewis T. Physiologically based pharmacokinetics modeling in the neonatal population-current advances, challenges, and opportunities. Pharmaceutics. 2023;15:2579.
40. Rowland M, Tozer TN. Clinical pharmacokinetics and pharmacodynamics: concepts and applications. Wolters Kluwer Health/Lippincott William & Wilkins; 2011.
41. Li Y, Dong N, Qin Y-X, Dai H-R, Hu Y-H, Zhao Y-T, et al. Therapeutic drug monitoring of perampanel in children diagnosed with epilepsy: focus on influencing factors on the plasma concentration-to-dose ratio. Epilepsia Open. 2022;7:737–46.
42. Jiménez-Fernández S, Gurpegui M, Correll CU, de Leon J, Schoretsanitis G. A systematic review of clozapine concentration-dose ratio from therapeutic drug monitoring studies in children and adolescents treated with clozapine for mental disorders. Ther Drug Monit. 2024;46:170–80.
43. Chen C, Xu T, Zhou K, Zhu S. Factors affecting voriconazole concentration to dose ratio changes according to route of administration. Eur J Hosp Pharm Sci Pract. 2023;31:31–5.
44. Tomizawa M, Hori S, Inoue K, Nishimura N, Nakai Y, Miyake M, et al. A low tacrolimus concentration-to-dose ratio increases calcineurin inhibitor nephrotoxicity and cytomegalovirus infection risks in kidney transplant recipients: a single-center study in Japan. Transplant Proc. 2023;55:109–15.
45. Chouchana M, Delage C, Godin O, Fontan J-E, Bellivier F, Gard S, et al. Factors associated with lamotrigine concentration/dose ratio in individuals with bipolar disorders. Eur Neuropsychopharmacol. 2023;73:75–81.
46. Marchette RCN, Carlson ER, Frye EV, Hastings LE, Vendruscolo JCM, Mejias-Torres G, et al. Heroin- and fentanyl-induced respiratory depression in a rat plethysmography model: potency, tolerance, and sex differences. J Pharmacol Exp Ther. 2023;385:117–34.
47. Waldhoer M, Bartlett SE, Whistler JL. Opioid receptors. Annu Rev Biochem. 2004;73:953–90.
48. Montandon G, Horner RL. Electrocortical changes associating sedation and respiratory depression by the opioid analgesic fentanyl. Sci Rep. 2019;9:14122.
49. Shook JE, Watkins WD, Camporesi EM. Differential roles of opioid receptors in respiration, respiratory disease, and opiate-induced respiratory depression. Am Rev Respir Dis. 1990;142:895–909.
50. Carbajal R, Eriksson M, Courtois E, Boyle E, Avila-Alvarez A, Andersen RD, et al. Sedation and analgesia practices in neonatal intensive care units (EUROPAIN): results from a prospective cohort study. Lancet Respir Med. 2015;3:796–812.
51. Quickfall D, Sklar MC, Tomlinson G, Orchanian-Cheff A, Goligher EC. The influence of drugs used for sedation during mechanical ventilation on respiratory pattern during unassisted breathing and assisted mechanical ventilation: a physiological systematic review and meta-analysis. eClinicalMedicine. 2024;68:102417.
52. Dahan A, Yassen A, Bijl H, Romberg R, Sarton E, Teppema L, et al. Comparison of the respiratory effects of intravenous buprenorphine and fentanyl in humans and rats. Br J Anaesth. 2005;94:825–34.
53. Lugli L, Garetti E, Goffredo BM, Candia F, Crestani S, Spada C, et al. Continuous fentanyl infusion in newborns with hypoxic–ischemic encephalopathy treated with therapeutic hypothermia: background, aims, and study protocol for time-concentration profiles. Biomedicines. 2023;11:2395.
54. Nimmo WS, Todd JG. Fentanyl by constant rate i.v. infusion for postoperative analgesia. Br J Anaesth. 1985;57:250–4.

55. Bardol M, Pan S, Walker SM, Standing JF, Dawes JM. Pharmacokinetic pharmacodynamic modeling of analgesics and sedatives in children. Paediatr Anaesth. 2023;33:781–92.
56. Bardol M, Norman E, Lagercrantz H, Fellman V, Standing JF. Fentanyl dosage for preterm infants suggested by a pharmacokinetic, -dynamic, and -genetic model. Pediatr Res. 2025;97:239–45.
57. Koehntop DE, Rodman JH, Brundage DM, Hegland MG, Buckley JJ. Pharmacokinetics of fentanyl in neonates. Anesth Analg. 1986;65:227–32.
58. Saarenmaa E, Neuvonen PJ, Fellman V. Gestational age and birth weight effects on plasma clearance of fentanyl in newborn infants. J Pediatr. 2000;136:767–70.
59. Singleton MA, Rosen JI, Fisher DM. Plasma concentrations of fentanyl in infants, children and adults. Can J Anaesth. 1987;34:152–5.
60. Gruber EM, Laussen PC, Casta A, Zimmerman AA, Zurakowski D, Reid R, et al. Stress response in infants undergoing cardiac surgery: a randomized study of fentanyl bolus, fentanyl infusion, and fentanyl-midazolam infusion. Anesth Analg. 2001;92:882–90.
61. Gauntlett IS, Fisher DM, Hertzka RE, Kuhls E, Spellman MJ, Rudolph C. Pharmacokinetics of fentanyl in neonatal humans and lambs: effects of age. Anesthesiology. 1988;69:683–7.
62. Norman E, Kindblom JM, Rane A, Berg A-C, Schubert U, Hallberg B, et al. Individual variations in fentanyl pharmacokinetics and pharmacodynamics in preterm infants. Acta Paediatr. 2019;108:1441–6.
63. Roth B, Schlünder C, Houben F, Günther M, Theisohn M. Analgesia and sedation in neonatal intensive care using fentanyl by continuous infusion. Dev Pharmacol Ther. 1991;17:121–7.
64. Collins C, Koren G, Crean P, Klein J, Roy WL, MacLeod SM. Fentanyl pharmacokinetics and hemodynamic effects in preterm infants during ligation of patent ductus arteriosus. Anesth Analg. 1985;64:1078–80.